

On the Interpretation of the Atmospheric Neutrino Data in Terms of Flavor Changing Neutrino Interactions

N. Fornengo, M. C. Gonzalez-Garcia and J. W. F. Valle¹

¹ *Instituto de Física Corpuscular – C.S.I.C.*

Departamento de Física Teórica, Universitat de València

46100 Burjassot, València, Spain

Abstract

Flavour changing (FC) neutrino–matter interactions have been proposed as a solution to the atmospheric neutrino anomaly. Here we perform the analysis of the full set of the recent 45 kTy Super-Kamiokande atmospheric neutrino data, including the zenith angle distribution of the contained events as well as the higher energy upward-going stopping and through-going muon events. Our results show that the FC mechanism can describe the data with a good level of statistical agreement. However when the zenith angle distribution of the through-going muon events is included the oscillation hypothesis provides a much better description. The combined analysis confines the amount of FC to be either maximal or to the level of about (10–20)%.

I. INTRODUCTION

Neutrinos produced as decay products in hadronic showers from cosmic ray collisions with nuclei in the upper atmosphere [1] have been observed by several detectors [2–8]. Although the absolute fluxes of atmospheric neutrinos are largely uncertain, the expected ratio (μ/e) of the muon neutrino flux ($\nu_\mu + \bar{\nu}_\mu$) over the electron neutrino flux ($\nu_e + \bar{\nu}_e$) is robust, since it largely cancels out the uncertainties associated with the absolute flux. In fact, this ratio has been calculated [1] with an uncertainty of less than 5% over energies varying from 0.1 GeV to 100 GeV. In this resides our confidence on the long-standing atmospheric neutrino anomaly.

Although the first iron-calorimeter detectors in Fréjus [2] and NUSEX [3] reported a value of the double ratio, $R(\mu/e) = (\mu/e)_{\text{data}}/(\mu/e)_{\text{MC}}$, consistent with one, all the water Cerenkov detectors Kamiokande [4], IMB [5] and Super-Kamiokande [6,7] have measured $R(\mu/e)$ significantly smaller than one. Moreover, the Soudan-2 Collaboration, also using an iron-calorimeter, reported a small value of $R(\mu/e)$ [8], showing that the so-called atmospheric neutrino anomaly was not a feature of water Cerenkov detectors.

Recent Super-Kamiokande high statistics observations [6,7] indicate that the deficit in the total ratio $R(\mu/e)$ is due to the number of neutrinos arriving in the detector at large zenith angles. Although e -like events do not present any compelling evidence of a zenith-angle dependence, the μ -like event rates are substantially suppressed at large zenith angles.

The $\nu_\mu \rightarrow \nu_\tau$ as well as the $\nu_\mu \rightarrow \nu_s$ [9,10] oscillation hypothesis provides a very good explanation for this smaller-than-expected ratio, which is also simple and well-motivated theoretically. This led the Super-Kamiokande Collaboration to conclude that their data provide good evidence for neutrino oscillations and neutrino masses [11]. However, alternative explanations to the atmospheric neutrino data have been proposed in the literature including the possibility of neutrino decay [12], the violation of relativity principles [13,14] or the violation of CPT symmetry [15]. These explanations, however, have been challenged by the precise data of Super-Kamiokande on upward going muon events [16,17] which allows to study the energy dependence of the neutrino survival (or disappearance) probability [18,19]. Based on such observations, both the possibility of an explanation of the anomaly in terms of neutrino decay [20] as well as the violation of relativity principles or the violation of CPT symmetry [19], have been disfavoured.

In Ref. [21] it was proposed an alternative explanation of the atmospheric neutrino data in terms of FC neutrino-matter interactions [22–27] and it was shown that even if neutrinos have vanishing masses and/or the vacuum mixing angle is negligible, FC neutrino matter interactions could explain the Super-Kamiokande results on contained events providing an excellent description to the data, statistically as good as neutrino oscillations.

In this paper we reanalyze the possibility of explaining the atmospheric neutrino anomaly by means of $\nu_\mu \rightarrow \nu_\tau$ conversion induced by flavour-changing neutrino-matter interaction which can be effective during the neutrino propagation in the Earth. We extend the analysis of Ref. [21] to the new set of Super-Kamiokande data by including also the up-going muon samples.

II. MASSLESS NEUTRINO EVOLUTION WITH FC INTERACTION

In our phenomenological approach we assume that the evolution equations which describe the $\nu_\mu \rightarrow \nu_\tau$ transitions in matter may be written as [23,25]

$$i \frac{d}{dr} \begin{pmatrix} \nu_\mu \\ \nu_\tau \end{pmatrix} = \sqrt{2} G_F \begin{pmatrix} 0 & \epsilon_\nu n_f(r) \\ \epsilon_\nu n_f(r) & \epsilon'_\nu n_f(r) \end{pmatrix} \begin{pmatrix} \nu_\mu \\ \nu_\tau \end{pmatrix}, \quad (1)$$

where $\nu_a \equiv \nu_a(r)$ ($a = \mu, \tau$) are the probability amplitudes to find these neutrinos at a distance r from their creation position, $\sqrt{2} G_F n_f(r) \epsilon_\nu$ is the $\nu_\mu + f \rightarrow \nu_\tau + f$ forward scattering amplitude and $\sqrt{2} G_F n_f(r) \epsilon'_\nu$ is the difference between the $\nu_\tau - f$ and $\nu_\mu - f$ elastic forward scattering amplitudes, with $n_f(r)$ being the number density of the fermions which induce such processes.

The parameters ϵ and ϵ' contain the information about FC neutrino interactions. Such FC interactions may be accompanied by neutrino mass [28] but this need not be the case [29,30]. One description would be to parametrize directly the FC interactions in terms of an effective four-fermion Hamiltonian. This could, for instance, arise by renormalization effects from the unification scale down to the electroweak scale in, say, supergravity models [30]. An alternative more phenomenological way is to consider the existence of a tree-level FC process $\nu_\alpha + f \rightarrow \nu_\beta + f$ where f is an elementary fermion (charged lepton or quark). The interaction can be mediated by a scalar or vector boson of mass m and the neutrino–fermion coupling is generically denoted by $g_{\alpha f}$ (α is a flavour index) and can be written as

$$\epsilon'_\nu = \frac{|g_{\tau f}|^2 - |g_{\mu f}|^2}{4m^2 \sqrt{2} G_F} \quad \text{and} \quad \epsilon_\nu = \frac{g_{\tau f} \cdot g_{\mu f}}{4m^2 \sqrt{2} G_F}. \quad (2)$$

Since we are assuming vanishing neutrino masses, the anti–neutrino transitions $\bar{\nu}_\mu \rightarrow \bar{\nu}_\tau$ are governed by the same evolution matrix given in Eq. (1). For the sake of simplicity, we consider $\epsilon_{\bar{\nu}} = \epsilon_\nu$ and $\epsilon'_{\bar{\nu}} = \epsilon'_\nu$, which implies that we have only two free parameters in the analysis. Moreover, we set our normalization on these parameters by assuming that the relevant neutrino interaction in the Earth is only with down-type quarks. One could also assume that the incoming atmospheric neutrino has FC interactions off-electrons or equivalently, due to charge neutrality, off-up-type quarks. For simplicity, in the present analysis we consider only the case of interactions on down-type quarks.

We have calculated the transition probabilities of $\nu_\mu \rightarrow \nu_\tau$ ($\bar{\nu}_\mu \rightarrow \bar{\nu}_\tau$) as a function of the zenith angle by numerically solving the evolution equation using the density distribution in [31] and a realistic chemical composition with proton/neutron ratio 0.497 in the mantle and 0.468 in the core [32].

III. FITTING THE DATA TO THE FC HYPOTHESIS

We have then used these probabilities to compute, as a function of the two parameters, ϵ_ν and ϵ'_ν , the theoretically expected numbers of events for the four sets of data reported by Super-Kamiokande: sub-GeV, multi-GeV stopping muons and through-going muons. The expected number of contained events are computed by convoluting the probability with the corresponding neutrino fluxes (for which we use the Bartol calculations [1]) and interaction

cross sections and taking into account the experimental efficiencies as detailed in Ref. [9]. For the up-going muon samples we obtain the effective muon fluxes for both stopping and through-going muons by convoluting the probabilities with the corresponding muon fluxes produced by the neutrino interactions with the Earth. We include the muon energy loss during propagation both in the rock and in the detector according to [33,34] and we take into account also the effective detector area for both types of events, stopping and through-going. We compute the effective area using the simple geometrical picture given in Ref. [35]. Our final results show good agreement with the full MC simulation of the Super-Kamiokande collaboration in the Standard Model case (see the thick solid line in Fig. 3).

In our statistical analysis we adopted the technique [9,36] of fitting separately the angular distributions of the μ - and e -like contained events (N_μ^i and N_e^i , i stands for sub-GeV and multi-GeV) and the up-going muon fluxes (Φ_μ^j , j = stopping, through-going). The expected number of events have been compared with the recent 45 kTy data reported by the Super-Kamiokande Collaboration [7,17,37] and the allowed regions in $(\epsilon_\nu, \epsilon'_\nu)$ have been determined from a χ^2 fit. In constructing the χ^2 function, we explicitly take into account the correlation of errors, both of theoretical and experimental origin. Details on the definition of the correlation matrix for contained events can be found in Ref. [9], while the definition of the sources of errors and their correlations for the up-going muons fluxes are given in Ref. [38,36]. Here we simply summarize that we consider the overall normalization of the up-going muon fluxes to be affected by an uncertainty of 20% but in order to account for the uncertainties in the primary cosmic ray flux spectrum we allow a 5% variation in the ratio between muon events in different energy samples. We further introduce a 10% theoretical error in the ratio of electron-type to muon-type events of the different samples. Uncertainties in the ratio between different angular bins are treated, similarly to Ref. [36], by allowing a variation of 5% times the difference between the mean bin cosines.

In Fig. (1) we show the contours of the regions allowed by the Super-Kamiokande data. The different panels of the figure refer to the fits performed over the different set of data separately: (a) sub-GeV; (b) multi-GeV; (c) stopping muons; (d) through-going muons. The shaded areas are the regions allowed at 90% C.L., while the dashed and dotted contours refer to 95 and 99 % C.L., respectively. The condition used to determine the allowed regions is: $\chi^2 = \chi^2_{min} + \Delta\chi^2$ where $\Delta\chi^2 = 4.6, 6.0, 9.2$ for 90, 95 and 99 % C. L., respectively.

The allowed regions for the contained events are, as expected, quite similar to the ones obtained in Ref. [21]. The individual best fits now improve with respect to the analysis of the old data: $\chi^2_{min} = 2.8/(8\,d.o.f.)$ for the sub-GeV data ($\epsilon_\nu = 0.180$ and $\epsilon'_\nu = 0.016$) and to $\chi^2_{min} = 5.4/(8\,d.o.f.)$ for the multi-GeV sample ($\epsilon_\nu = 0.186$ and $\epsilon'_\nu = 0.154$). The combination of the two sets of contained events leads to allowed regions which are very close to the one reported in the Ref. [21] and which are not reproduced again here. Instead, in Fig.1, we show the regions which are allowed by the up-going muons sample of Super-Kamiokande. Panel (c) stands for stopping muons and panel (d) for the through-going sample.

In the case of stopping muons, we see that, analogously to the contained events, the allowed region lies in the sector of the plane where the average survival probability is of the order of a half, which is what appears to be needed for explaining the data. Instead, in the case of through-going muons, the experimental data do not show such a strong reduction with respect to the theoretical calculations, and therefore the allowed region lies in the

upper-left corner of the parameter space, which refers to a smaller transition probability. In both cases, the best fit point for each individual sample is very good: $\chi^2_{min} = 0.5/(3\,d.o.f.)$ for stopping muons ($\epsilon_\nu = 0.286$ and $\epsilon'_\nu = 0.104$) and $\chi^2_{min} = 4.4/(8\,d.o.f.)$ for the through-going case ($\epsilon_\nu = 0.035$ and $\epsilon'_\nu = 0.123$). Both for the contained and for the up-going events, the best fits have the same level of statistical confidence as compared to the oscillation interpretation of the atmospheric neutrino data. This is shown in Table I, where we report the best fit values we obtain for the different data sets in the case of the FC- ν interactions scenario and in the case of the neutrino oscillation scenario [38].

The allowed regions can be qualitatively understood in the approximation of constant matter density. The conversion probability in this case is

$$P(\nu_\mu \rightarrow \nu_\tau) = \frac{4\epsilon_\nu^2}{4\epsilon_\nu^2 + \epsilon'^2_\nu} \sin^2\left(\frac{1}{2}\eta L\right), \quad (3)$$

where $\eta = \sqrt{4\epsilon_\nu^2 + \epsilon'^2_\nu} \sqrt{2}G_F n_f$. For $n_f = n_d \approx 3n_e$ and $\epsilon'_\nu < \epsilon_\nu$, the oscillation length in matter is given by

$$L_{osc} = \frac{2\pi}{\eta} \approx 1.2 \times 10^3 \left[\frac{2 \text{ mol/cc}}{n_e} \right] \left[\frac{1}{\epsilon_\nu} \right] \text{ km.} \quad (4)$$

From Eq. (3) one can see that in order to have a relatively large transition probability, as required by the contained events and, also, by the stopping muons events, the FC parameters are required to be in the region $\epsilon'_\nu \lesssim \epsilon_\nu$ and $\eta \gtrsim \pi/R_\oplus$. This last condition leads to a lower bound on ϵ_ν . The island in Fig. 1.(b) corresponds to $\eta \sim \pi/R_\oplus$.

The combination of the different data sets in a single χ^2 -analysis is shown in Fig. 2. Panel (a) shows the combination of the full angular distribution of contained events with the total (unbinned) event rate of stop and through-going muons data, while panel (b) refers to the combination of all the angular distributions, including that of through-going muon events. In Fig. 2(a) the information brought by the higher energy data is effective at the normalization level, since no information about their angular dependence is included. In this case the allowed region is confined to two relatively small areas, one which contains the best fit point $\epsilon_\nu = 0.077$ and $\epsilon'_\nu = 0.074$ ($\chi^2_{min} = 15.1/(20\,d.o.f.)$) and which extends down towards small values of the FC parameters, and one region which refers to parameters in the (0.1-0.2) range for both ϵ_ν and ϵ'_ν . We notice that in this case the best fit point is close to the secondary best fit case obtained in Ref. [21] for the combined analysis of the contained events.

However, as seen in Fig. 2(b), when the angular information of both stopping and through-going muons is included in the data analysis, the situation gets problematic, mainly due to the angular distribution of the through-going data set. The allowed regions now form a set of isolated 'islands', two of them referring to values of the FC parameters of the order of 0.1-0.2, while the other allowed region requires close-to-maximal FC parameters. This region contains the best fit point at $\epsilon_\nu = 0.79$ and $\epsilon'_\nu = 1$ acceptable at the 90 % CL ($\chi^2_{min} = 42/(33\,d.o.f.)$). The secondary minima are: $\epsilon_\nu = 0.12$ and $\epsilon'_\nu = 0.24$ ($\chi^2_{min} = 46/(33\,d.o.f.)$) and $\epsilon_\nu = 0.056$ and $\epsilon'_\nu = 0.112$ ($\chi^2_{min} = 47/(33\,d.o.f.)$).

The behaviour of the allowed regions can be understood by observing Fig. 3 where we show the angular distributions for the four cases: (a) sub-GeV; (b) multi-GeV; (c) stopping

muons; (d) through-going muons. We show the distributions for the best fit point obtained from the combination of contained events with the total number of upward going stopping muons $P_1 = (\epsilon_\nu, \epsilon'_\nu) = (0.077, 0.074)$ and for the best fit point obtained from the analysis of the full data set $P_2 = (0.79, 1)$. Although both points give a similar normalization to the up-going muon data samples, point P_1 gives a better description to the angular dependence of the contained events, but it does not describe well the zenith angle distribution of the through-up-going muon events. As commented above, such point correspond to an effective FC-oscillation length of the order of the Earth radius. In this case we can see the imprints of the “oscillatory” sine behaviour in the expected angular distribution of the up-through-going muon events. Such behaviour, however, does not appear to be present in the Super-Kamiokande data, leading to a worse overall fit. In the case of multi-GeV contained events, this oscillatory behaviour is averaged out due to the smaller angular resolution in the data and point P_1 can give a good description of the data. Point P_2 , on the other hand, gives a worse description of the contained events but fits better the upward going muon data, with the exception of the last two angular bins where it does not produce a sufficient amount of through-going muons at angles $0 < \theta < 15$ degrees below the horizon.

IV. DISCUSSION

What can we say about the required strength of the neutrino-matter interaction in order to obtain a good fit of the observed data? From our best fit results and Eq. (2) we see that for masses $m \approx 200$ GeV we need the combination of couplings $g_{\tau f} \cdot g_{\mu f}$ and $|g_{\tau f}|^2 - |g_{\mu f}|^2$ to be of the order of 2. (We notice that in the case of our best fit point of Fig. 2(a), the above combination need to be almost one order of magnitude lower, i.e. 0.2–0.3). Model independent constrains on the ϵ parameter can be extracted from their contribution to the ν_μ neutral current cross section measured at low energy [39]. This limit is stronger for interactions with quarks due to the better precision of the $\sigma_{NC,N}^{\nu_\mu}$ data compared to the $\sigma_{NC,e}^{\nu_m u}$. We have estimated that they constrain $\epsilon \lesssim \mathcal{O}(0.1)–\mathcal{O}(1)$ depending on the fermion f coupled to the neutrino. No limit on the ϵ' parameter can be obtained from these measurements. In this way, the FC interactions could be ruled out as the *only* source of the modification of the atmospheric neutrino predictions with respect to those of the Standard Model. Nevertheless, although not required by the data, which admit a very good interpretation in terms of standard ν_μ to ν_τ oscillations, they could still be there at some level. This is theoretically not an *ad hoc* assumption from the point of view that in many models neutrino masses naturally co-exist with FC-neutrino interactions.

On the other hand, one may turn the argument the other way around: should the atmospheric neutrino anomaly be explained in terms of neutrino oscillations, then it will be possible to use the non-observation of an additional effect in the atmospheric neutrino data in order to impose new model independent limits on the strength of the ϵ and ϵ' parameters, as can be foreseen by looking at Fig. 1(d).

In summary, we have shown that flavour changing ν_μ -matter interactions can describe the full data of Super-Kamiokande on atmospheric neutrinos with a reasonable level of statistical agreement. However, once all the upward going muon zenith angle distribution data are included, the oscillation hypothesis provides a much better description. The combined analysis moreover requires the amount of FC to be either close to maximal or at the level of

about (10–20)%. This worsening is partly due to the fact that in this scenario the transition probability is energy independent while the data shows a smaller conversion for the higher energy up-through-going muon events. Moreover the data shows an angular dependence which is in contradiction with the expectations from FC-neutrino interaction for neutrinos arriving at angles above 15 degrees below the horizon.

The above FC mechanism can be further tested at future Long Baseline experiments. From Eq. (3), using $n_e \sim 2$ mol/cc, we get that for $\epsilon \simeq \epsilon' \sim 1$ (0.1) for the planned K2K experiment [40] one gets $P(\nu_\mu \rightarrow \nu_\tau) \sim 0.35$ (0.004) while for MINOS [41] one finds $P(\nu_\mu \rightarrow \nu_\tau) \sim 0.75$ (0.04).

ACKNOWLEDGMENTS

We thank R. Vazquez for providing us with the program to compute the muon energy loss. We are also grateful to S. Nussinov for pointing us out the limits from the neutrino neutral current measurements. M.C. G-G is grateful to the Instituto de Fisica Teorica from UNESP and to the CERN Theory division for their kind hospitality during her visits. This work was supported by Spanish DGICYT under grant PB95-1077 and by the European Union TMR network ERBFMRXCT960090.

REFERENCES

- [1] L. V. Volkova, Sov. J. Nucl. Phys. **31**, 784 (1980); M. Honda *et al.*, Phys. Rev. **D52**, 4985 (1995); V. Agrawal *et al.*, *ibid* **D53**, 1314 (1996); T. K. Gaisser and T. Stanev, *ibid* **D57**, 1977 (1998).
- [2] K. Daum *et al.* Z. Phys. **C66**, 417 (1995).
- [3] M. Aglietta *et al.*, Europhys. Lett. **8**, 611 (1989).
- [4] H. S. Hirata *et al.*, Phys. Lett. **B280**, 146 (1992); Y. Fukuda *et al.*, *ibid* **B335**, 237 (1994).
- [5] R. Becker-Szendy *et al.*, Phys. Rev. **D46**, 3720 (1992).
- [6] Y. Fukuda *et al.*, Phys. Lett. **B433**, 9 (1998); Phys. Lett. **B436**, 33 (1998).
- [7] M. Messier, talk at APS Meeting of the Division of Particles and Fields (DPF 99), Los Angeles, CA, 5-9 Jan 1999.
- [8] W. W. M. Allison *et al.*, Phys. Lett. **B449**, 137 (1999).
- [9] M. C. Gonzalez-Garcia, H. Nunokawa, O. L. G. Peres, T. Stanev and J. W. F. Valle, Phys. Rev. **D58**, 033004 (1998); M.C. Gonzalez-Garcia, H. Nunokawa, O.L. Peres and J. W. F. Valle, Nucl. Phys. **B543**, 3 (1999), hep-ph/9807305.
- [10] R. Foot, R. R. Volkas and O. Yasuda, Phys. Rev. **D58**, 013006 (1998); O. Yasuda, Phys. Rev. **D58**, 091301 (1998); G. L. Fogli, E. Lisi, A. Marrone, G. Scioscia, Phys. Rev. **D59**, 033001 (1999), hep-ph/9808205; E.Kh. Akhmedov, A.Dighe, P. Lipari and A.Yu. Smirnov, Nucl. Phys. **B542**, 3 (1999), hep-ph/9808270.
- [11] Y. Fukuda *et al.*, Phys. Rev. Lett. **81**, 1562 (1998).
- [12] V. Barger, J.G. Learned, S. Pakvasa, and T.J. Weiler, Phys. Rev. Lett. **82**, 2640 (1999).
- [13] M. Gasperini, Phys. Rev. **D38**, 2635 (1988); J. Pantaleone, A. Halprin, C.N. Leung, Phys. Rev. **D47**, 4199 (1993); A. Halprin, C.N. Leung, J. Pantaleone Phys. Rev. **D53**, 5365 (1996).
- [14] S. Coleman, S. L. Glashow, Phys. Lett. **B405**, 249 (1997); S. L. Glashow, A. Halprin, P.I. Krastev, C.N. Leung, J. Pantaleone, Phys. Rev. **D56**, 2433 (1997).
- [15] S. Coleman, S. L. Glashow, Phys. Rev. **D59**, 116008 (1999).
- [16] Y. Fukuda *et al.*, Phys. Rev. Lett. **82**, 2644 (1999).
- [17] A. Habig *et al.*, talk at APS Meeting of the Division of Particles and Fields (DPF 99), Los Angeles, CA, 5-9 Jan 1999, hep-ex/9903047. (1978), *ibid* **D20**, 2634(1979).
- [18] P. Lipari, M. Lusignoli Phys. Rev. **D60**, 013003 (1999).
- [19] G.L. Fogli, E. Lisi, A. Marrone, G. Scioscia, hep-ph/9904248.
- [20] G.L. Fogli, E. Lisi, A. Marrone, G. Scioscia, Phys. Rev. **D59**, 117303 (1999).
- [21] M.C. Gonzalez-Garcia, M.M. Guzzo, P.I. Krastev, H. Nunokawa, O.L.G. Peres, V. Pleitez, J.W.F. Valle and R. Zukanovich Funchal, Phys. Rev. Lett. **82**, 3202 (1999).
- [22] L. Wolfenstein, Phys. Rev. **D17**, 2369
- [23] J. W. F. Valle, Phys. Lett. **B199**, 432 (1987).
- [24] M. Fukugita, T. Yanagida, Phys. Lett. **B206**, 93 (1988).
- [25] M. M. Guzzo, A. Masiero and S. Petcov, Phys. Lett. **B260**, 154 (1991); E. Roulet, Phys. Rev. **D44**, 935 (1991).
- [26] V. Barger, R. J. N. Phillips and K. Whisnant, Phys. Rev. **D44**, 1629 (1991); P. I. Krastev and J. N. Bahcall, hep-ph/9703267; S. Bergman, Nucl. Phys. **B515**, 363 (1998).
- [27] E. Ma and P. Roy, Phys. Rev. Lett. **80**, 4637 (1998).
- [28] J. Schechter and J. W. F. Valle, Phys. Rev. **D22**, 2227 (1980).

- [29] R. Mohapatra, J. W. F. Valle, Phys. Rev. D34, 1642 (1986); D. Wyler and L. Wolfenstein, Nucl. Phys. B218, 205 (1983).
- [30] L. J. Hall, V. A. Kostelecky and S. Raby, Nucl. Phys. **B267** 415 (1986); Y. Okada, hep-ph/9809297.
- [31] A. M. Dziewonski and D. L. Anderson, Phys. Earth and Planet. Interiors, **25**, 207 (1981).
- [32] J. Bahcall and P. Krastev, Phys. Rev. **C56**, 2839 (1997).
- [33] W. Lohmann, R. Kopp and R. Voss, CERN Yellow Report EP/85-03.
- [34] E. Zas, F. Halzen, R.A. Vazquez, Astropart. Phys. **1** 297 (1993).
- [35] P. Lipari, M. Lusignoli Phys. Rev. **D58**, 073005 (1998).
- [36] G. Fogli and E. Lisi, Phys. Rev. **D52**, 2775 (1995); G. Fogli, E. Lisi, D. Montanino and G. Scioscia, *ibid* **D55**, 485 (1997); G.L. Fogli, E. Lisi, A. Marrone, G. Scioscia, Phys. Rev. **D59**, 033001 (1999).
- [37] M. Messier, private communication.
- [38] N. Fornengo, M.C. Gonzalez-Garcia and J.W.F. Valle, in preparation.
- [39] C. Caso et al, The European Physical Journal **C3** (1998) 1.
- [40] C. Yanagisawa *et al.*, in *Physics Beyond the Standard Model: from Theory to Experiment*, World Scientific, 1998 (ISBN-981-02-3638-7) Eds. I. Antoniadis, L. E. Ibanez and J. W. F. Valle.
- [41] D. Michael *et al.*, Nucl Phys. B, Proc. Suppl. **66**, 432 (1998).

Data	d.o.f	χ^2_{minFC}	χ^2_{minOsc}
sub-GeV	8	2.8	3.1
multi-GeV	8	5.4	5.4
Contained	18	10.	8.7
Stopping- μ	3	0.5	0.4
Through-Going- μ	8	4.4	3.5
Contained + total up- μ	20	15.	9.
Contained + angular up- μ	33	42.	15.

TABLE I. χ^2_{min} obtained for several data combinations in the framework of FC- ν interactions as compared to the case of the neutrino vacuum-oscillation scenario.

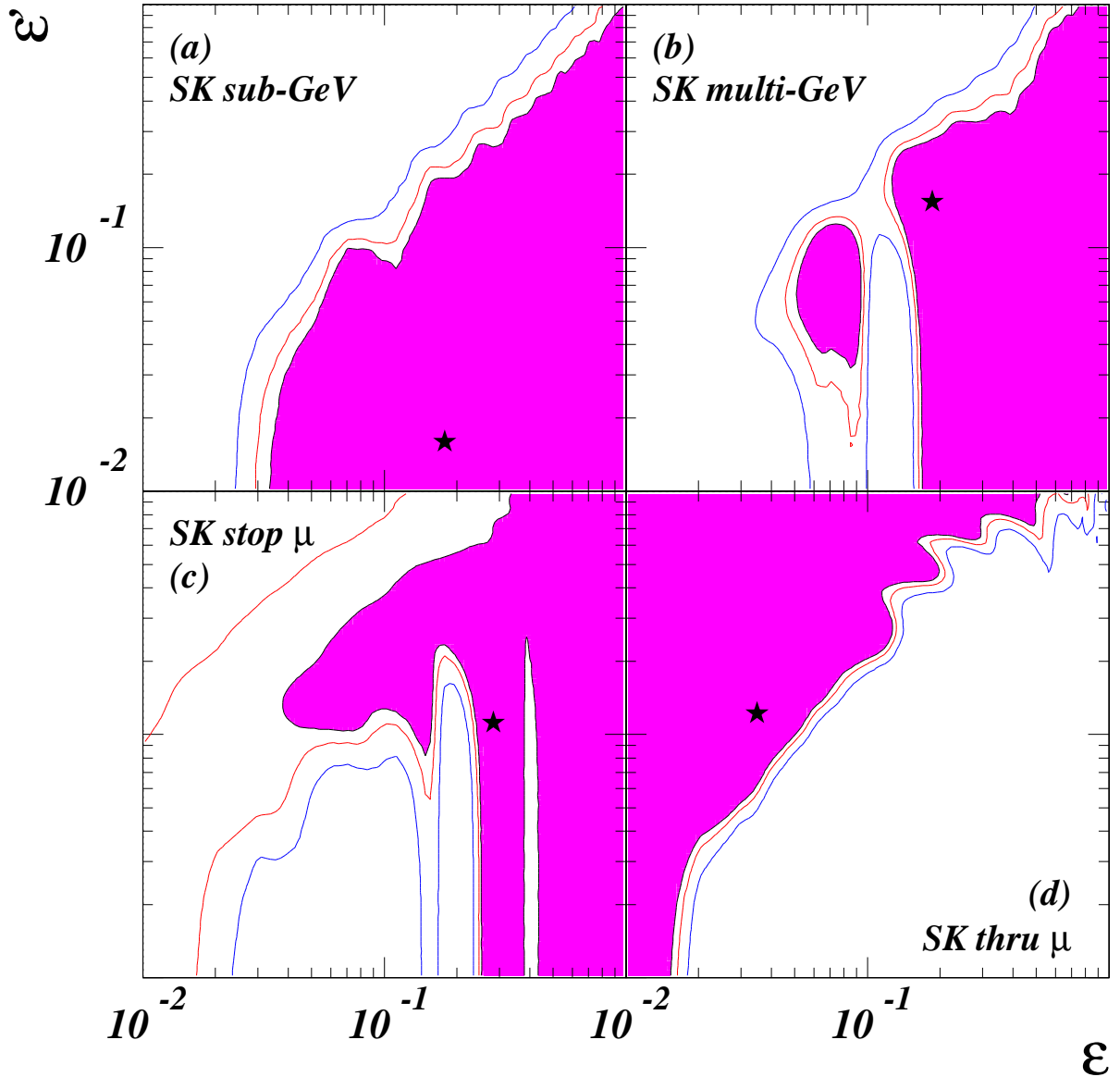


FIG. 1. Allowed regions for ϵ_ν and ϵ'_ν for Super-Kamiokande (a) sub-GeV, (b) multi-GeV, (c) stopping muons and (d) through-going muons in the FC massless-neutrino scenario. The best fit points for each case are indicated by stars. The shaded area refers to the 90% C.L.. while the contours stand for 95% and 99% C.L.

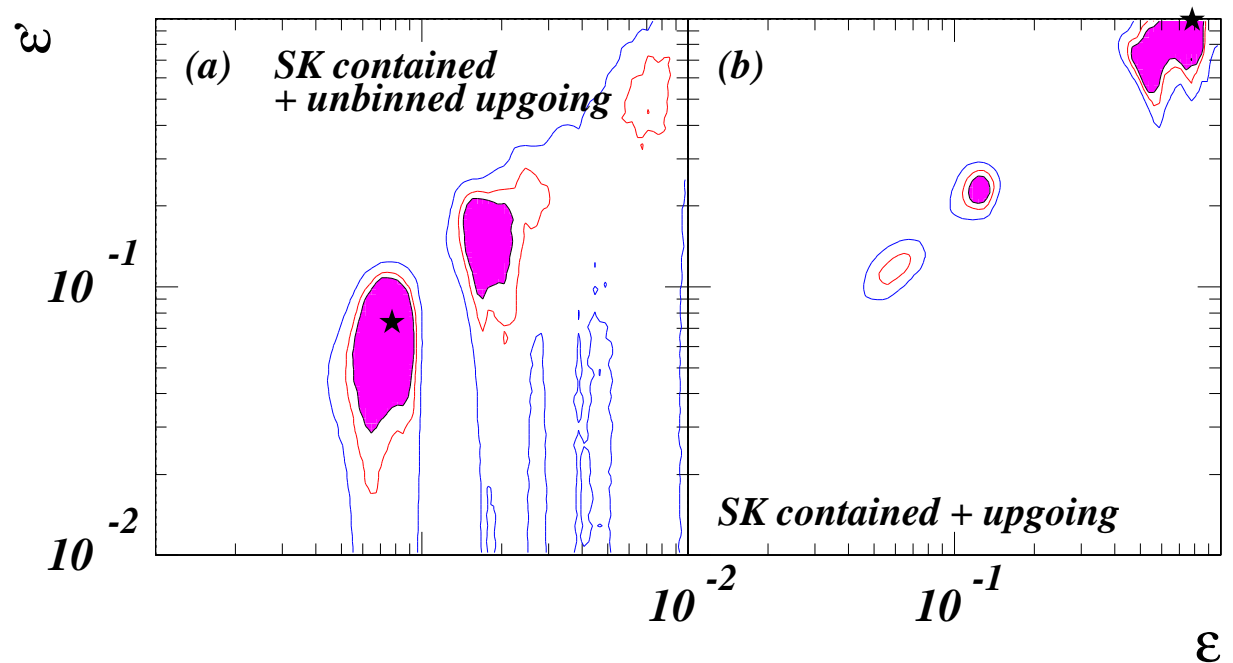


FIG. 2. Allowed regions for ϵ_ν and ϵ'_ν for the combination of the Super-Kamiokande data sets: (a) the binned contained events are combined with total (unbinned) up-going events; (b) binned contained and total events. The best fit points for each case are indicated by stars. The shaded area refers to the 90% C.L. while the contours stand for 95% and 99% C.L.

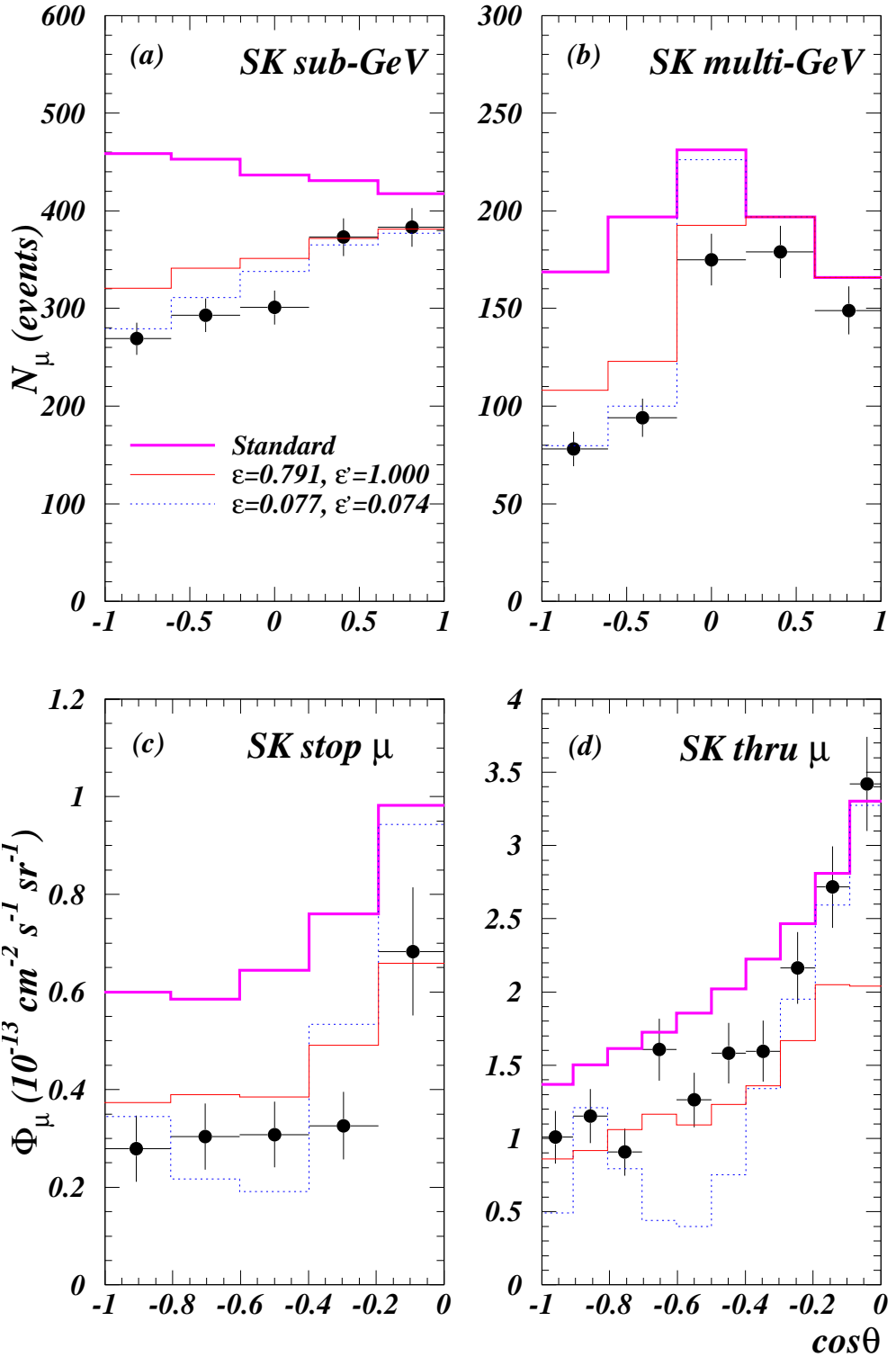


FIG. 3. Best-fit zenith angle distributions in the massless-neutrino FC scenario. The thick-solid lines corresponds to the calculation in absence of new physics. The dotted line corresponds to the best fit point obtained by the analysis of the contained events combined with total (unbinned) up-going events. The thin-solid line is for the best fit point of the combined analysis of contained and up-going muon events. The 45 kTy Super-Kamiokande data are indicated by crosses.